Chemical Engineering Science 86 (2013) 124–136

Contents lists available at SciVerse ScienceDirect

Chemical Engineering Science

journal homepage: www.elsevier.com/locate/ces

Spout fluidized beds: Recent advances in experimental and numerical studies

Vinayak S. Sutkar, Niels G. Deen*, J.A.M. Kuipers

Multiphase Reactors Group, Department of Chemical Engineering and Chemistry, Eindhoven University of Technology, P.O. Box 513, 5600 MB Eindhoven, The Netherlands

HIGHLIGHTS

- Spout-fluidized beds are compared to spouted beds and fluidized beds.
- An overview of spout-fluidized bed experimentation is given.
- An overview of spout-fluidized bed modeling is given.

GRAPHICAL ABSTRACT

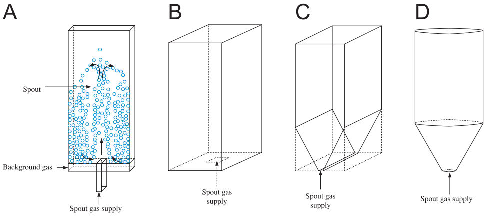

ARTICLE INFO

Article history:
Received 3 November 2011
Received in revised form
23 May 2012
Accepted 14 June 2012
Available online 23 June 2012

Keywords:
Spout fluidized beds
Flow regime map
Multiphase flow
Fluidization
Particle processing
Granulation

ABSTRACT

In the past few decades, the applicability of spout fluidized beds has been augmented immensely. This is not only due to the fact that these systems combine characteristics of spouted and fluidized beds but also to their efficacy to handle chemical transformations involving simultaneous heat and mass transfer in combination with varying particles size. This is important in applications such as granulation, coating, drying, pyrolysis and combustion etc. The present work aims at critically analyzing the recent advances in experimental and numerical studies of spout fluidized beds. Initially, the discussion will concentrate on experimental studies emphasizing variation of minimum spouting and spout-fluidizing velocity, operating pressure, mixing and jet penetration length. Furthermore, flow regime maps will be discussed. Subsequently, the application of various numerical modeling strategies is highlighted. Also, recommendations are given for future work required in experimental and modeling studies.

© 2012 Elsevier Ltd. All rights reserved.

1. Introduction

Fluidized beds for gas–solid contacting have often proven to be more attractive than other contactor configurations, which is due to the unique characteristics such as enhanced heat and mass transfer rates, high mixing rates and uniform reaction conditions. In spite of these characteristics, for economical operation the applicability of fluidized beds is limited to small particle sizes (diameter in the range of a few hundred micrometers). Inspired by this limitation, Mathur and Gishler (1955) developed the spouted bed which effectively deals with coarse particles (diameter in the range of few millimeters) with same efficacy as a conventional fluidized bed. In this bed, a high velocity gas stream flows through a orifice or spout (generally 25 times the particle diameter) located at the bottom of the bed, which results in generation of a local high velocity region in the center (referred to as spout) and a region with down flow of particles along the bed walls (referred to as annulus). So, in the spout particles move in a structured manner in the vertical direction (with little radial displacement) accompanied by void (bubble) propagation. This subsequently leads to high circulation rates, which are proportional to the gas flow rate, leading to flexible operation. In spite of these advantages, some problems arise during operation: the spout features highly depend on the inlet gas flow rate. Mathur and Gishler (1955) performed experiments in two spouted beds with spout diameters in the range of 0.95–1.27 cm and reported that spout generation was observed in a narrow range of gas flow rates. Apart from this narrow range for spout generation, Nagarkatti and

---

* Corresponding author. Tel.: +31 40 2473681; fax: +31 40 2475833.
E-mail address: N.G.Deen@TUe.nl (N.G. Deen).

0009-2509/$ - see front matter © 2012 Elsevier Ltd. All rights reserved.
http://dx.doi.org/10.1016/j.ces.2012.06.022

Chatterjee (1974) reported that high flow rates are required for spout generation, which results in lower contact times in the spout. Furthermore, minor particle movement is observed in the radial direction. Particles enter the spout radially at the bottom and leave at the top in the fountain region and subsequently move downward in the annulus to enter the spout for the next circulation cycle. This results in non-uniform distribution of operating conditions. Mathur and Gishler (1955) have determined the variation of flow rate, solids circulation rate and pressure drop in a cylindrical bed and reported that, at a certain height (0.2 m from the bottom), very low particle velocities prevail in the annulus as compared to the spout (exceeding 6 m/s). In addition, they also reported that this non-uniformity in particle velocity remains unaffected in both the regions at increased gas velocity.

Mostly experiments were carried in cylindrical beds equipped with conical or rectangular bottom sections with varying cross sectional area. In spite of these expansions, the formation of dead zones were reported at the intersection. This results in reduced mixing. Also, it is evident that, the selection of other operating parameters such as inlet flow rate, bed aspect ratio, spout dimension and physical properties of the particles plays an imperative role in spout formation. Small changes in these parameters can result in remarkable changes in spout properties and bed behavior. Hence, spouted beds have rarely been used in applications involving substantial changes in physical and/or chemical properties. By considering this, Chatterjee (1970) proposed a novel gas–solid contactor, compromising unified features of both fluidized and spouted beds, known as spout fluidized bed or spout-fluid bed. Although, both names are used in literature, from now on we will refer to these apparatus as spout fluidized beds. In these beds an additional background gas (also known as auxiliary or fluidizing gas) is supplied through the bottom as compared to the conventional spouted bed. Fig. 1 depicts various configurations of spout fluidized beds.

Some of the distinguishing features of spout fluidized beds are:

1. Additional background gas flow leads to higher circulation and mixing rates, due to the bubble generation in the annulus, leading enhanced particle movement in vertical and radial directions.
2. The total flow rate required to fluidize particles is lower in comparison to fluidized and spouted beds. This is mainly attributed to cross flow of additional background gas supply. This argument was supported by Chatterjee (1970) who performed experiments using sand particles (of average diameter equal to 1.08 mm) in a cylindrical bed. He reported that approximately 36% lower gas flow rate (algebraic summation of minimum spouting and minimum background flow rate) was required in a spout fluidized bed as compared to a spouted bed.
3. Due to the uneven distribution of the gas at a certain distance from the distributor plate, a narrow operational range has been observed for fluidized and spouted beds, which often suffer from slugging behavior, whereas in spout fluidized beds wider flow rates can be used with a lower tendency to slugging. This provides a wider operational range, specifically for particles with varying size and density.

Cui and Grace (2008) reviewed the applicability of spouted beds for treatment of organic materials by characterizing the various bed configurations with available correlations for minimum spouting velocity, pressure drop etc. They also presented a comprehensive comparison of fluidized beds with spouted beds based on various criteria. In Table 1 we have summarized the main features of fluidized and spouted beds, reported by Cui and Grace (2008) and included our observations for spout fluidized beds.

There are several examples where spout fluidized beds have been successfully applied in various chemical applications using different bed geometries. Few important applications are mentioned here: municipal solid waste (MSW) gasification (Thamavithya and Dutta, 2008); biomass steam gasification for production of Syngas (Xie et al., 2010); chemical looping combustion of coal (Shen et al., 2010); catalytic partial oxidation of methane (Marschall and Mleczko, 2000). Furthermore, spout fluidized beds attracted attention in converting agriculture waste streams into energy through combustion. Albina (2006) investigated the emission properties (generation of CO and CO_2) after combustion of rice husk in multi spouted and spout fluidized beds. Moreover, torrefaction of agriculture residues in spout fluidized beds such as rice husks, sawdust, peanut husks, bagasse with water hyacinth in nitrogen to improve combustion properties of fuel has been reported by Pimchuai et al. (2010). Xiao et al. (2007) studied the partial gasification of high ash Chinese coal in pilot plant. Other applications involve coating of porous aero gel particles (Plawsky et al., 2010) and coating of tablets (Kfuri and Freitas, 2005). In addition, Kfuri and Freitas (2005) reported additional features of spout fluidized beds for pharmaceutical application. Furthermore, spout fluidized beds have actively been used in applications involving simultaneous heat and mass transfer, such as in drying of Guava seeds (Osorio-Revilla et al., 2004); biopolymers as Xanthan gum (Ciro-Velásquez et al., 2010); mango pulp (Lopes da Cunha et al., 2006); residue of olive oil (pomace) at low temperature (Marmo, 2007); carrots (Zielinska and Markowski, 2007; Białobrzewski et al., 2008). Other miscellaneous applications include dry premixing of sand and cement to produce mortar in pilot plant (Plawsky et al., 2003; Park et al., 2006) and

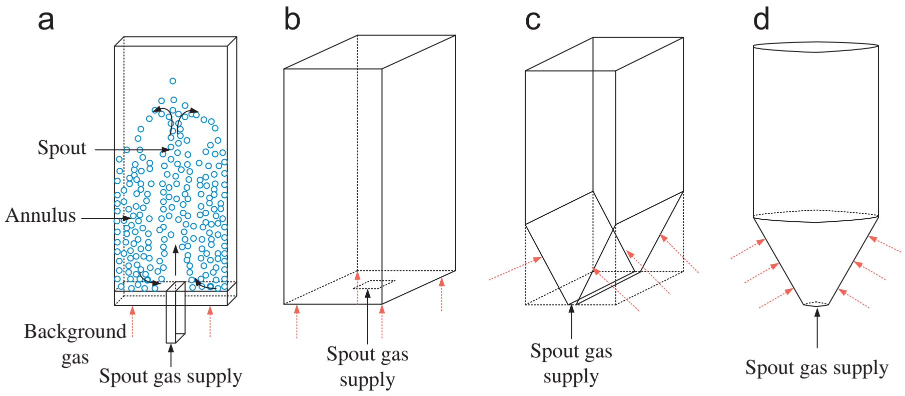

Fig. 1. Schematic representation of different spout fluidized bed contactors: (a) pseudo 2D (b) rectangular (c) slotted rectangular and (d) cylindrical spout fluidized beds. The dotted arrows indicate the positions and angles of the background gas supply.

Table 1
Comparison of fluidized beds, spouted beds and spout fluidized beds.

Property	Fluidized bed	Spouted bed	Spout fluidized bed
Mean particle size	$\sim$0.3–3 mm; usually <1 mm	$\sim$0.6–6 mm; usually >1 mm	$\sim$1.0–3.0 mm; usually >1 mm
Particle size distribution	Usually broad	Usually narrow	Usually broad
Pressure drop/height within the bed	96–100% of that needed to support the particles, $\sim(\rho_s-\rho_g)g(1-\varepsilon)$	Less than 75% of that needed to support the weight of the particles, i.e. $<0.75\ (\rho_s-\rho_g)g(1-\varepsilon)$	Lower than spouted and fluidized beds and highly influenced by background flow
Pressure drop across entry orifices	Usually 30–50% of that across the bed	As small as possible consistent with satisfying the other constraints, e.g. $d_{orifice}<25d_{p,mean}$	As small as possible consistent with satisfying the other constraints, e.g. $d_{orifice}<25d_{p,mean}$
Axial gradient of pressure	Virtually independent of height in the column	Varies with height	Highly depends on bed height
Temperature gradient	Very uniform temperature over entire fluidized bed	Significant temperature gradients both axially and radially	Uniform temperature over cross-section of the bed
Column geometry	Usually cylindrical columns	Usually diverging conical base with or without cylindrical portion above	Usually cylindrical, square or rectangle either with conical or flat bottom section
Orifice diameter	No restriction	Must not exceed 25 times of mean particles diameter	Must not exceed 25 times of mean particles diameter
Gas motion	Less ordered; depends on flow regime and specific geometry	Outwards from the spouts into the dense phase, except just above inlet	Outwards in spout and annulus for flat bottom
Particle motion	Complex flow regimes and particle motion. Region surrounding the gas entry orifices is usually fluidized with few particle–particle contacts	Systematic circulation patterns, up the spout and slowly downward in the annulus. Annulus is moving packed bed flow with substantial particle–particle contacts	Systematic circulation patterns with upward motion of particles from spout and slowly downward in annuls with radial displacement of particles from annulus to spout
Particle segregation	Very little segregation providing that particles are well fluidized	Significant segregation according to both size and density of particles	Significant segregation according to both size and density of particles
Attrition	Normally little except in cyclone or jet regions	Significant in spout region and in fountain above	Significant in spout region and in fountain above
Bed depth	Broad range of depths, e.g. from 0.1 to 20 m dense bed depth	More limited range of depths, usually between 0.2 and 2.0 m	Broad range of depths, e.g. from 0.1 to 50 m dense bed depth
Superficial gas velocity	Broad range, typically: $u-u_{mf}=0.2-10\ m/s$	More limited range, typically: $1-1.8u_{ms}$	Typically in the range of $1-1.8u_{ms}$ and depends on background velocity
Orifice velocity variation	Some variation with time across each individual orifice as bubbles form and leave the orifice or jet	Essentially steady as flow is controlled to each hole from an upstream valve	Essentially steady as flow is controlled to each hole from an upstream valve
Internals	Common in fluidized bed processes	Rare in spouted bed processes, except for some use of draft tubes and heat transfer coils	Draft tubes are commonly used

hydraulic transport of glass particles in water (Littman et al., 2009). Anabtawi et al. (2003,2004) have extended the applicability of spout fluidized beds to three phase systems.

The present work highlights the recent advances in characterizing hydrodynamics of spout fluidized beds emphasizing the discussion on pressure drop, minimum spouting and spout fluidizing velocity, mixing behavior and jet penetration length. Furthermore, the effects of variation of spout and background velocity on the prevailing flow patterns is discussed with the aid of flow regime maps. Also, we provide an overview of the developments in modeling studies applied to spout fluidized beds. Recently, Zhong et al. (2011) presented an excellent review discussing the main features of spout fluidized beds. The current paper aims to build on that review and add a critical discussion of the main reactor features in relation to operation, design and scale-up, with recommendations for practical use. In addition, we give a brief review of the numerical modeling approaches and their strong and weak points for the description of spout fluidized beds.

2. Experimental studies

The dynamic behavior of gas–solid spout fluidized beds has been studied extensively. The effect of various operating parameters on the overall flow characteristics is often represented with flow regime maps. In this section, we discuss the correlations for minimum spout velocity, minimum spout-fluidizing velocity, pressure drop variations and jet penetration length, along with recent developments to obtain flow regime maps.

2.1. Minimum spouting velocity and minimum spout-fluidization velocity

The minimum spouting velocity is one of the important properties to study the hydrodynamic behavior of spouted and spout fluidized beds, which is defined as the superficial gas velocity through the spout inlet at the inception of a spout, without considering particle movement in the annulus. This quantity can be determined by measuring the variation of pressure drop with superficial spout velocity. As the spout velocity increases, the pressure drop also increases linearly until it reaches a maximum value, after which it decreases dramatically up to a certain velocity and then remains constant. The value of the velocity at maximum pressure drop is known as the minimum spout velocity. Zhang et al. (2010) have investigated the minimum spout velocity both experimentally and numerically in a 2D spout fluidized bed (with dimensions $W\times D\times H=0.1\times 0.03\times 0.5\ \mathrm{m}^3$ and a spout inlet of $0.01\times 0.03\ \mathrm{m}^2$) by measuring the variation of pressure drop with

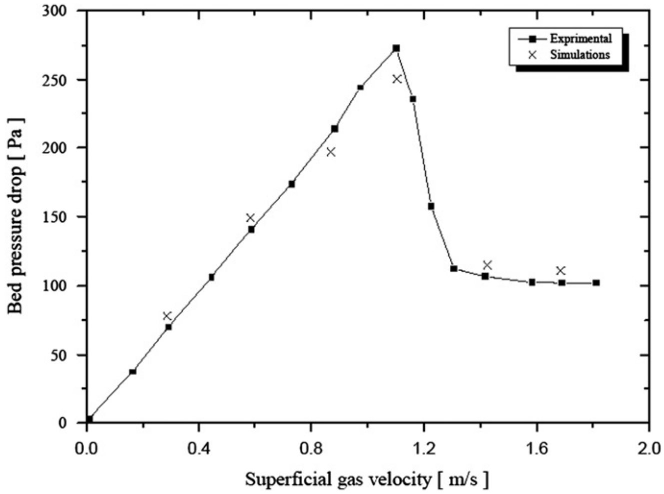

Fig. 2. Variation of bed pressure drop with superficial gas velocity in a 2D spout fluidized bed (with dimensions $W\times D\times H=0.1\times 0.03\times 0.5$ m^3 and a spout inlet of 0.01×0.03 m^2) by using polypropylene beads (with 2.8 mm diameter and 900 kg/m^{3}density) (Zhang et al., 2010).

polypropylene beads (of 2.8 mm in diameter). There results showed good agreement between experimental and numerical data as shown in Fig. 2. These results indicate a minimum spout velocity of 1.1 m/s at maximum pressure drop of 280 Pa.

Mathur and Gishler (1955) studied the effect of bed height, column and spout diameter and physical properties of the particles on the minimum spouting velocity. Their results revealed that there is a linear relationship between the superficial gas velocity and the bed height. This contradicts with the behavior of conventional fluidized beds, where a variation in the gas flow is independent of the bed height. Moreover, this variation is highly influenced by the bed diameter and given by:

$$u_{ms}=\left(\frac{d_p}{D_c}\right)\left(\frac{D_s}{D_c}\right)^{1/3}\left(\frac{2gH_b(\rho_s-\rho_g)}{\rho_g}\right)^{1/2} \tag{1}$$

The above equation was derived for cylindrical spouted beds. Nagarkatti and Chatterjee (1974) proposed a correlation Eq. (2) for the calculation of the minimum spout-fluidizing velocity by extending the correlation developed by Lefroy and Davidson (1969) and Mathur and Gishler (1955). They also considered the cross flow due to the additional background gas supply and the effect of bed height, inlet spout diameter and cone angle:

$$u_{msf}=\left(\frac{d_p}{D_c}\right)\left(\frac{D_s}{D_c}\right)^{1/3}\left(\frac{2gH_b(\rho_s-\rho_g)}{\rho_g}\right)^{1/2}+\frac{d_p^2(\rho_s-\rho_g)g}{150}\frac{\varepsilon_m^3}{1-\varepsilon_m}(1-\phi)$$

$$\phi=0.24d_p^{-0.32}D_s^{0.235}H_b^{0.16} \tag{2}$$

where ϕ depends on the geometry of the bottom section of the bed. This correlation is valid for conical distributors with a cone angle of 60°. The effect of the cone angle is lumped into the constant 0.24.

Anabtawi et al. (1992) performed experiments in spouted and spout fluidized beds with a rectangular base (of dimensions $W\times D\times H=0.1\times 0.05\times 0.2$ m^3) by varying the physical particle properties and reported that previous correlations developed for spouted systems are not applicable for spout fluidized beds. They proposed the following correlations for minimum spouting velocity, minimum spout-fluidizing velocity and minimum spout fluidizing flow rate:

$$u_{ms}=2.44\left(\frac{d_p}{D_c}\right)^{0.7}\left(\frac{D_s}{D_c}\right)^{0.58}\left(\frac{H_b}{D_c}\right)^{0.5}\left(2gH_b\left(\frac{\rho_s-\rho_g}{\rho_g}\right)\right)^{0.28} \tag{3}$$

$$u_{msf}=2.44\left(\frac{d_p}{D_c}\right)^{0.7}\left(\frac{D_s}{D_c}\right)^{0.58}\left(\frac{H_b}{D_c}\right)^{0.5}\left(2gH_b\left(\frac{\rho_s-\rho_g}{\rho_g}\right)\right)^{0.28}+u_{mf}(1-\phi) \tag{4}$$

$$Q_{msf}=0.098\left(\frac{d_p}{D_c}\right)^{0.7}\left(\frac{D_s}{D_c}\right)^{0.58}\left(\frac{H_b}{D_c}\right)^{0.5}\left(2gH_b\left(\frac{\rho_s-\rho_g}{\rho_g}\right)\right)^{0.28}+Q_{mf}(1-\phi)$$

$$\phi=3.66\times10^{-5}D_s^{0.104}d_p^{-0.485}H_b{}^{-0.656}Q_{0,msf}^{-1.3} \tag{5}$$

Zhong et al. (2006b) defined the minimum spout-fluidized velocity as the minimum superficial gas velocity for the inception of a spout and fluidization in the annulus. Furthermore, they proposed a correlation for the minimum spouting velocity and the minimum spout-fluidizing velocity by incorporating the effect of background velocity as follows:

$$u_{ms}=24.5(2gH_b)^{0.5}\left(\frac{d_p}{W_c}\right)^{0.472}\left(\frac{W_s}{W_c}\right)^{0.183}\left(\frac{H_b}{W_c}\right)^{0.208}\left(1+\frac{u_{bg}}{u_{mf}}\right)^{-0.284}\left(\frac{\rho_s-\rho_g}{\rho_g}\right)^{0.225}\quad u_{bg}\geq 0 \tag{6}$$

$$u_{msf}=1.65(2gH_b)^{0.5}\left(\frac{d_p}{W_c}\right)^{0.465}\left(\frac{W_s}{W_c}\right)^{0.264}\left(\frac{H_0}{W_c}\right)^{0.178}\left(\frac{u_{bg}}{u_{mf}}\right)^{0.172}\left(\frac{\rho_s-\rho_g}{\rho_g}\right)^{0.273}\quad u_{bg}>0 \tag{7}$$

Another correlation for the minimum spout fluidized velocity was reported by Jin et al. (2000), who considered the effect of operating pressure. This correlation is given as follows:

$$u_{msf}=4.29\left(\frac{d_p}{D_c}\right)^{1.05}\left(\frac{D_s}{D_c}\right)^{1/3}\left(\frac{p}{p_0}\right)^{-0.5}\left(\frac{2gH_b(\rho_s-\rho_g)}{\rho_g}\right) \tag{8}$$

To estimate the parameter dependencies during complex behavior of spout fluidized beds, linear fitting such as least square method will not always yield precise results. Therefore some authors applied advanced nonlinear analysis techniques such as an artificial neural network or a support vector machine (SVM). Wang et al. (2011) performed experiments to investigate the effect of various parameters on the minimum spout-fluidized velocity by using a least square vector machine (LS-SVM). In this method, the effect of the investigated parameters is related to the minimum spout fluidized velocity. With their approach the relative error in the results decreased. The main observations were:

1. The minimum spout-fluidizing velocity increases with increasing bed height. This is mainly attributed to the fact that as the bed height increases the static load and distribution surface area also increase resulting in higher momentum losses.
2. The minimum spout-fluidizing velocity also increases with spout diameter. This is due to the fact that, as the diameter of spout increases, the amount of particles entering from the annulus also increases, requiring higher drag to displace the particles.
3. As the background velocity increases, the minimum spout-fluidization velocity decreases. This is because, as the amount of background gas increases in the annulus, the porosity decreases, so the solids become loosely packed, leading to a reduced resistance for the spout gas to pass through.
4. In addition Zhong et al. (2008) investigated the effect of the operating parameters on the minimum spouting velocity at elevated pressure and revealed that variations were highly dependent on the operating pressure.

Similar variations have been reported for variation of the minimum spout-fluidizing velocity with bed height, particle diameter for spout fluidized beds (Zhong et al., 2006a), spouted beds (Pianarosa et al., 2000; Bi, 2004) and spout-fluidized beds with a draft tube (Xu et al., 2009).

Wang et al. (1999) proposed a correlation for spouted beds with a draft tube by extending the approach reported by Mathur and Gishler (1955). Initially, in this correlation the minimum spout velocity was calculated without background flow and then corrected with a term to account for the effect of the background velocity as

$$u_{msDT} = u_{msDT,0} + k u_{bg} \tag{9}$$

$$u_{msDT,0} = 1.975\left(\frac{d_p}{D_c}\right)\left(\frac{D_{DT}}{D_c}\right)^{0.33}\left(\frac{2gH_b(\rho_p-\rho_g)}{\rho_g}\right)^{0.5}\left(\frac{R}{H_b}\right)^{0.78}\left(\frac{D_{DT}}{D_c}\right)^{0.2} \tag{10}$$

On a similar basis, Zhang (2005) proposed a correlation for spout fluidized beds with a flat bottom by taking into account the effect of the immersed draft tube and superficial background gas velocity as follows:

$$\frac{u_{msDT}}{u_{mf}} = 5.674\left(\frac{D_{DT}}{D_c}\right)^{0.245}\left(\frac{R}{D_c}\right)^{0.119}\left(\frac{L_{DT}}{D_c}\right)^{0.752} \times\left(\frac{H_b}{D_c}\right)^{-0.397}\left(\frac{(u_{mf}-u_{bg})}{u_{mf}}\right)^{0.186} \tag{11}$$

Xu et al. (2009) performed experiments in a spout fluidized bed of 0.12 m diameter with a centrally placed draft tube ($D \times H = 0.025\ \mathrm{m} \times 0.2\ \mathrm{m}$) with Silica gel particles (of 1.2 mm in diameter) and investigated the effect of the background flow rate, spout diameter and static bed height on the minimum spout velocity and proposed the following correlation:

$$u_{msDT} = 1.338\left(\frac{d_p}{D_c}\right)\left(\frac{D_s}{D_c}\right)^{0.33}\left(\frac{2gH_b(\rho_p-\rho_g)}{\rho_g}\right)^{0.5} \times\left(\frac{R}{D_c}\right)^{0.282}\left(\frac{H_b}{D_c}\right)^{-0.096}\left(1-\frac{u_{bg}}{u_{mf}}\right)^{0.592}. \tag{12}$$

2.2. *Pressure variation in spout fluidized bed*

The investigation of hydrodynamic behavior of gas–solid systems often involves measurements of the pressure history. This provides practical information about series of events (after applying a suitable sampling method) occurring during operation with relatively ease. Information on generation, merging and collapse of bubbles can be obtained. Moreover, fluctuations in the gas flow rate can also be captured through the pressure signal. There are number of articles published such as Cheremisinoff (1986), Yates and Simons (1994), Louge (1997), Werther (1999) who comprehensively reviewed the available techniques for measurement of pressure drop, solids volume fraction, particle velocity and mass flow rate in fluidized beds. van Ommen and Mudde (2007) discussed recent advances in the development of various measurement techniques such as capacitance and optical probes, tomography and pressure measurements, mainly related to gas–solid fluidization, with emphasis on guidelines to minimize the error encountered during pressure drop measurement. Mathur and Gishler (1955) reported that pressure drop in spouted beds is the result of frictional losses, acceleration of particles, generation and collapse of bubbles. Zhong et al. (2006b) measured the pressure drop in a rectangular spout fluidized bed (with dimensions $W \times D \times H = 0.3 \times 0.03 \times 2\ \mathrm{m}^3$) for various particles such as Mung beans, polystyrene, Millet and glass beads using a pressure sensor. Zhong et al. (2006b) reported results for three different modes of operation:

1. In the first operational mode, only spout gas is introduced into the bed. At low superficial spout gas velocity, the total pressure drop is directly proportional to the spouting velocity up to certain value, after which it decreases. When the gas velocity increases, the pressure drop also increases to overcome the static bed load (the spout velocity is still lower than the minimum fluidization velocity). Once the minimum fluidization velocity is reached, the pressure drop starts decreasing whilst a spout is being formed, followed by a dramatic decrease in pressure drop, which does not depend on the gas velocity. Similar behavior was reported for spouted beds by Epstein and Grace (1996).
2. In the second operational mode, only background gas is used to fluidize the bed. In this case, the pressure drop also increases with superficial gas velocity and then remains constant (minimum fluidization condition).
3. In the third mode, background gas and spout gas are combined. In this case, the pressure drop increases linearly with the spout velocity (for Mung beans of aspect ratio equal to 1.33 at a constant background velocity of 0.39 times the minimum fluidization velocity) and subsequently decreases to a constant value. A similar kind of variation has been observed in the spout and annular regions, with reduced maximum pressure drop in the annulus, approximately at the same spout and background velocities. Different behavior was reported for varying background velocity (at constant spout velocity). As the background velocity increases, the pressure drop in the spout remains constant (about 1.4 kPa), whereas in the annulus it increases up to background velocities of 0.5 m/s and then fluctuates around a value of about 1.2 kPa. These fluctuations are related to the generation and collapse of bubbles.

Detailed analysis of the variation of pressure signals provides information about dynamic behavior of gas–solid systems and its impact on reactor performance. Several authors analyzed the obtained pressure signal using statistical analysis (Xu et al., 2004), fast Fourier transformation (Link et al., 2005; Gryczka et al., 2008, 2009), chaotic analysis (Ellis et al., 2003), fractal analysis (Fan et al., 1993) and Wavelet analysis (Lu and Li, 1999). Using recent advances in signal analysis, Zhong and Zhang (2005b) analyzed the measured pressure signal at various locations in a spout fluidized bed by Shannon entropy analysis and quantified the effect of the variation of the spout and background velocities on the measured pressure. Their measurements revealed that the Shannon entropy has a very distinct behavior depending on the combination of spout and background velocities. Hence, it can be used for the construction of flow regime maps. Furthermore, Zhong and Zhang (2005c) reported a new signal processing method to analyze the time dependent pressure signal by using an auto regressive model (ARM) to obtain a power spectrum. Link et al. (2008) have successfully studied the hydrodynamic behavior of a 3D gas–solid spout fluidized bed (dimensions $W \times D \times H = 0.15 \times 0.08 \times 1\ \mathrm{m}^3$) with a flat bottom, by using the nonintrusive positron emission particle tracking (PEPT). In this technique, the motion of a single active particle has been tracked in the entire domain. In a similar way van Buijtenen et al. (2011b) applied PEPT technique to quantify the behavior of multi spout-fluidized beds.

Finally we mention here some of our recent results related to the variation of pressure drop in a 2D spout fluidized bed (dimensions $W \times D \times H = 0.14 \times 0.02 \times 1\ \mathrm{m}^3$, and spout dimensions of $0.01\ \mathrm{m} \times 0.02\ \mathrm{m}$) with a centrally located draft tube (dimensions $W \times D \times H = 0.05 \times 0.02 \times 0.32\ \mathrm{m}^3$) obtained by using two pressure sensors located 0.02 m from the bottom of the bed in the spout and annulus respectively. The bed was initially filled with 1 mm glass beads up to 0.14 m bed height and the spout and background velocities were varied. The resulting pressure drop profiles are presented in Figs. 3 and 4 respectively.

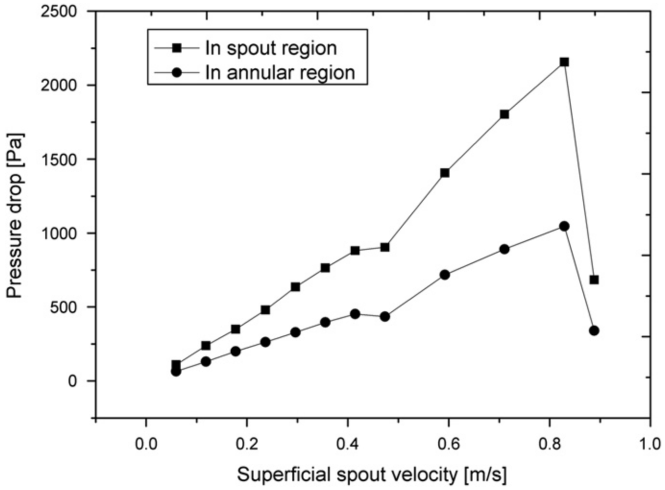

Fig. 3. Variation of pressure drop for 1 mm glass beads (of 2526 kg/m^3 density) with superficial spout velocity in the spout and annulus of a 2D spout fluidized bed (dimensions $W \times D \times H = 0.14 \times 0.02 \times 1$ m^3, and spout dimensions of 0.01 m × 0.02 m) with a centrally located draft tube (dimensions $W \times D \times H = 0.05 \times 0.02 \times 0.32$ m^3).

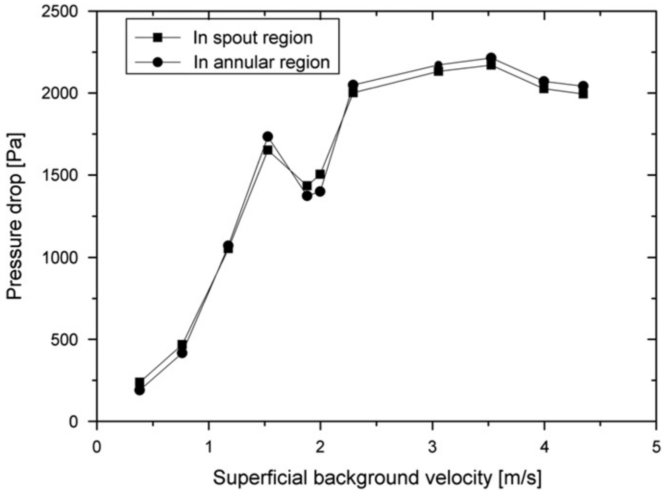

Fig. 4. Variation of pressure drop for 1 mm glass beads (of 2526 kg/m^3 density) with superficial background velocity in the spout and annulus of a 2D spout fluidized bed (dimensions $W \times D \times H = 0.14 \times 0.02 \times 1$ m^3, and spout dimensions of 0.01 m × 0.02 m) with a centrally located draft tube (dimensions $W \times D \times H = 0.05 \times 0.02 \times 0.32$ m^3).

As the superfical spout gas velocity increases, pressure drop in the spout and annulus increases linearly up to 0.8 m/s and then decreases dramatically. However, on the other hand, increasing the superficial background velocity results in increased pressure drop up to 2.5 m/s and then remains constant. It follows that small changes in spout and/or background velocity result in considerable variation in pressure drop in both the spout and the annulus up to some spout and background velocities.

2.3. Gas and particle mixing

In gas–solid systems the heat and mass transfer rates are highly influenced by the extent of mixing and solids circulation. Inadequate mixing often results in dead zones in the bed, which lead to hot spots or cold spots, i.e. areas with little or no reaction. So, good mixing in gas–solid–liquid systems is desirable, but difficult to achieve over the entire operational range. Zhang et al. (2008,2009a,b,2011), Zhong et al. (2006a,c,2007a,2010) and Jin et al. (2009) quantified mixing in spout fluidized bed by using various techniques. Mixing methods can be classified into static and dynamic methods, depending on the method of analysis applied. In static methods, the mixing is analyzed for a certain time, either by image processing or by some other means, whereas in dynamic methods mixing is analyzed at any given time interval. The latter methods can further be subdivided into intrusive and non-intrusive. In intrusive methods, the system is seeded with a suitable tracer such as NO_2, CO_2 or phosphorus etc. In non-intrusive methods, analysis is carried out without disturbing the system, e.g. by visual observation, image processing (e.g. Saadevandi and Turton, 1998), positron emission particle tracking and an electromagnetic method.

Note that, overall gas mixing occurring in spout fluidized bed can be divided into two types of mechanisms such as diffusion and convection (circulation and bubble formation and collapse). Mixing due to diffusion and particle circulation is mainly encountered at low spout and background velocities, whereas formation and collapse of bubbles plays an imperative role at higher velocities.

Zhong et al. (2006c) investigated the mixing in a spout fluidized bed ($D \times H = 0.3 \times 2$ m) by seeding two tracer gases, namely carbon monoxide (CO) and sulfur dioxide (SO_2) in the spout and annulus respectively and measuring the concentrations at certain distances form the injection point. They reported very distinct mixing features which are summarized as:

1. At a low aspect ratio ($H/D = 0.67$): as the background velocity increases in the spout and annulus the CO concentration decreases and the SO_2 concentration increases. This indicates that higher amount of SO_2 is transferred from the annulus to the spout. Moreover, as the spout gas velocity increases, the CO concentration in the spout decreases, whereas the SO_2 concentration increases. The opposite behavior in concentration profiles was reported for the annulus. This indicates that, a higher gas transfer rate occurred from the annulus to the spout.
2. At a high aspect ratio ($H/D = 1$): as the background velocity increases, the CO concentration in the spout region decreases and the SO_2 concentration increases. However, the extent of increase is lower near the wall. This is because the bubbles that are formed in the annulus travel to the spout and then collapse. Hence an increased SO_2 concentration is observed. As the aspect ratio increases further, the same CO and SO_2 concentrations are found in the radial direction, which indicates good bed mixing. Furthermore, as the spout velocity increases the concentration of CO increases and SO_2 decreases, which implies a lower radial penetration of gas from the annulus.

Zhang et al. (2008) reported a method to investigate the mixing in a spout fluidized bed by combining image processing and the bed-frozen method. In this method, the concentration of tracer particles at given time and space is determined by subsequently stopping the spout and background gas supply and simultaneously inserting a frame box, which allows determination of the location of tracer particles in the bed. This study revealed that, the initial locations of the tracer particles do not affect the obtained mixing. The applicability of this method is limited due to the fact that it requires considerable time for separation and counting of tracer particles at each section of the frame box and simultaneously stopping and inserting the frame box is cumbersome to achieve.

Jin et al. (2009) investigated the effect of physical properties and operating parameters on the mixing in a pseudo 2D spout fluidized bed using three tracer particles with specific color and different density, namely Silica gel, Mung and glass and reported similar results as Zhong et al. (2010).

In addition, Zhong et al. (2010) also quantified the cycle and residence time distribution in a spout fluidized beds by using above mentioned method and reported that:

1. Generation of circulation patterns highly depends on the density of the particles. As the density increases, the mean cycle time decreases.
2. Increase in the spout and background gas velocities results in reduction of the circulation time. However, a non-uniform residence time distribution has been observed with increasing spout velocity at fixed background velocity, which is due to the fact that as the spout velocity increases particles near the wall move slowly with longer trajectories as compared to particles in the spout. Based on this study, they also proposed the particle circulation pattern in bed, which is schematically shown in Fig. 5.

Zhong et al. (2007a) quantified the effect of operating parameters on mixing time and reported similar trends in variation.

Zhang et al. (2011) proposed a novel method to investigate the mixing in a spout fluidized bed with polymer particles (of 2.8 mm diameter and 900 kg/m^3 density) and analyzed the effect of operating parameters by considering the change in Shannon entropy. In this the bed is seeded with tracer particles and heated with a microwave source. Their trajectories are captured by using an infrared camera. Based on these studies, a correlation was proposed to describe the mixing time as

$$P = 1 - \exp - 0.548 u_g^{0.48} \rho^{*0.43} t \tag{13}$$

P is the ratio of the Shannon entropy increase at a certain location to the maximum possible entropy increase at the mixing equilibrium state ($P = S^*/S^*_e$). u_g is the mean gas velocity, ρ^* is the ratio of tracer density to the particle density and t is time. The applicability of this method is limited to laboratory scale systems with a total solid content of a few kilogram and additionally it is difficult to have tracer particles with the same physical properties as the primary solids. Börner et al. (2011) investigated the particle re-circulation and residence time for active (under influence of liquid spray) and inactive zones (not influenced by liquid spray) in four contactors (with the same bed dimensions) namely fluidized, spout-fluidized (with and without draft plate) and spouted beds. They obtained particle velocity fields and local solids volume fraction distributions from particle image velocimetry (PIV) and digital image analysis (DIA) respectively and combined those to calculate particle flux fields. Experiments were performed by varying the superficial background and spout velocities for 1.8 mm alumina particles. This study revealed that:

1. Spout fluidized bed: as the superficial gas velocity increases, the residence time in the active zone increases, while at constant superficial gas velocity as the spout flow rate increases the residence time in the active zone decreases. This is because at increasing superficial gas velocity the gas-particle drag also increases the bubbling action (the spout starts to swing in alternating directions). The formed bubbles may also restrict particles entering the spout from the annulus, leading to higher mixing.
2. Spout fluidized bed with draft plates: as the superficial gas velocity increases the residence time in the active zone slightly decreases or remains constant, however with a lower magnitude as compared to the case without draft plates. The insertion of draft plates results in reduction of radial movement of particles, where the spout residence time is highly influenced by the dimension of plates.

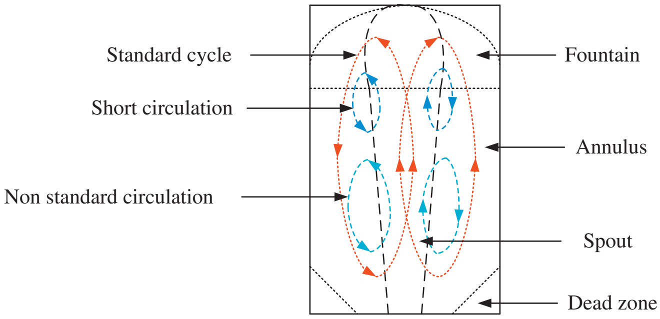

Fig. 5. Representation of circulation pattern in a spout fluidized bed (of dimensions $W \times D \times H = 0.1 \times 0.03 \times 0.3$ m^3) with 2.8 mm polymer particles of 900 kg/m^{3}density (Zhong et al., 2010).

van Buijtenen et al. (2011a) have investigated the effect of collision properties on the bed dynamics for glass, γ-alumina oxide and zeolite 4A particles. They used particle image velocimetry (PIV) and digital image analysis (DIA), which yielded instantaneous particle velocity fields and solid volume fraction fields respectively for selected regimes, viz. spout fluidization, jet-in-fluidized-bed and spouting-with-aeration regimes. This study conclusively showed significant variations in solid volume fractions for each particle type. Unstable spout generation has been observed for γ-alumina oxide and zeolite 4A particles in the intermediate or spout fluidization regime and in the spouting-with-aeration regime. Zhong et al. (2006d) have performed experiments in rectangular spout-fluidized bed and revealed that the selection of background gas is equally important to influence the flow pattern generation which ultimately determines the degree of mixing.

2.4. Jet penetration length

The jet penetration length is defined as the distance at which spontaneous change in the bed characteristics is observed, depending on the generation and collapse of formed bubbles. Knowlton and Hirsan (1980) classified the jet penetration length in three types namely (i) length of bed achieved just before the bubble collapse (ii) length at which series of bubbles are formed and (iii) minimum length at which there is permanent formation of small cavities near the spout. More discussion about this issue can be found in Filla et al. (1983) and Bi (2004).

Apart from visual and photographic analysis, there are other methods that can be used to quantify the jet penetration length in fluidized beds such as optical and capacitance probes, radiation dosimeters and pressure measurements. However, the applicability of these methods has rarely been tested for spout fluidized beds. Zhong and Zhang (2005a) applied combination of visual observations, pressure measurements and digital image analysis to explore the jet variation and penetration length depending on operating parameters. They proposed the following correlation:

$$\frac{L_j}{D_s} = 10.86\,(\mathrm{Fr})^{0.39}\left(\frac{H_b}{D_c}\right)^{-0.17}\left(\frac{u_g}{u_{mf}}\right)^{-0.11}(\mathrm{Re}_p)^{-0.03} \quad 0 \le u_g < 3u_{mf}$$

$$\mathrm{Fr} = \frac{\rho_g}{\rho_s - \rho_g}\frac{u_{sp}^2}{gD_s} \quad \text{and} \quad \mathrm{Re}_p = \frac{d_p \rho_g u_{sp}}{\mu_g}. \tag{14}$$

2.5. Regime map

The hydrodynamic behavior of spout fluidized beds not only depends on the operating parameters (spout and background velocity) but also on the physical–chemical properties of both phases (size, shape and density of the solids, as well as viscosity, density and humidity of the gas) and bed configuration (bed height, spout diameter and cone angle). Small changes in these parameters can dramatically change the overall bed behavior. So, it is of great practical use to construct a flow regime map/phase diagram that is valid over the entire operational range to indentify distinct flow patterns and regime transitions. There are several occasions in which flow regime maps have been successfully applied for gas–solid operations, however without background gas, that is either in fluidized or spouted beds. Additional background gas substantially changes the flow pattern, which needs to be accounted for. Flow regime maps are generally constructed by maintaining one of the gas velocities constant and changing another. The background velocity is generally maintained to a certain value and variation of the flow pattern has been observed by gradually increasing the spout velocity.

Apart from visual observations, a number of other methods can be used to construct the flow regime map, such as pressure fluctuations, bed height, high-speed images and velocity analysis. Recently, Oliveira et al. (2008) constructed the flow regime map for semi-cylindrical spouted beds by using a pressure sensor. The data were analyzed by various techniques viz. statistical analysis, mutual information theory, spectral and Hurst's Rescaled Range methods. In addition, there are other methods such as deterministic chaos, and the Wigner distribution, whose applicability yet needs to be tested for spout fluidized beds. Link et al. (2005) and van Buijtenen et al. (2011b) quantified the flow regime map for respectively a 3D spout fluidized bed (of dimensions $W \times D \times H = .154 \times 0.084 \times 1\ \mathrm{m}^3$ with 4 mm glass beads and spout dimension of $0.022\ \mathrm{m} \times 0.012\ \mathrm{m}^2$) and a multiple spout fluidized bed (of dimensions $W \times D \times H = 0.45 \times 0.02 \times 2.5\ \mathrm{m}^3$ with 3 mm glass beads and three identical spout of size $0.01 \times 0.02\ \mathrm{m}^2$) by visual observations, digital image recordings, FFT of the pressure signal, positron emission particle tracking and particle image velocimetry. The obtained flow regime map for the 3D spout fluidized bed and multiple spout fluidized bed are shown in Figs. 6 and 7 respectively.

The overview of studies on flow regime map construction for spout fluidized is given in Table 2 supplemented with details about the experimental set up and applied techniques.

From the experimental studies it has become clear that the flow transitions are highly sensitive to operating conditions and very complex to analyze. However, Dogan et al. (2000) reported that the transition between flow regimes mainly involves symmetric and asymmetric instabilities. These instabilities may arise due to the growth of surface disturbances, occurring due to revolution of the spout axis (dancing of spout) and distribution of gas both in the spout and the annulus. Also spout termination can cause surface disturbances. However, Zhong et al. (2006b,d) reported that in spout fluidized beds the transitions are mainly caused by bubble formation near the wall, which highly depends on the background gas. Based on the previous analysis, the following important considerations and recommendations in development of flow regime maps are made:

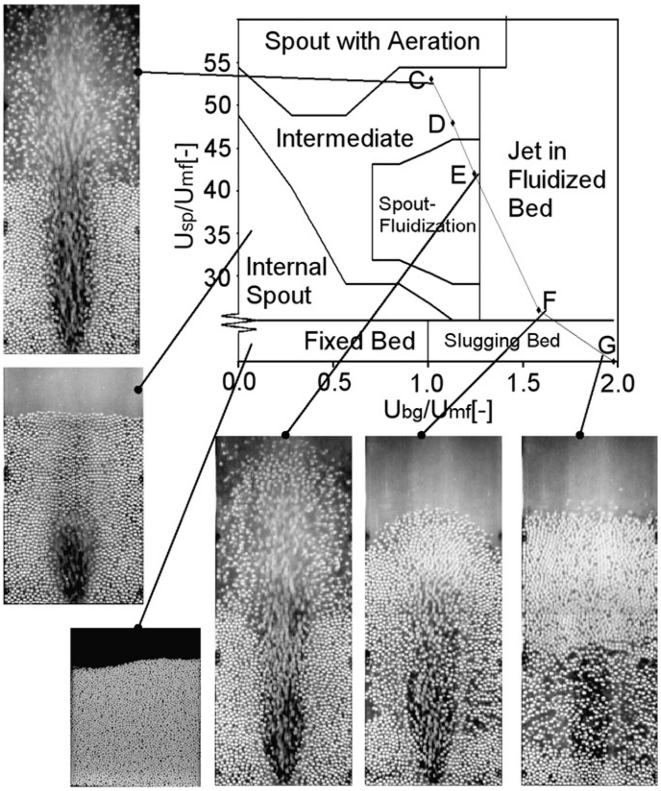

Fig. 6. Flow regime map of 3D spout fluidized bed (of dimensions $W \times D \times H = 0.154 \times 0.084 \times 1\ \mathrm{m}^3$ and spout dimension of $0.022\ \mathrm{m} \times 0.012\ \mathrm{m}^2$) by using 4 mm glass beads with variation in background (u_{bg}) and spout velocity (u_{sp}) (Link et al., 2005).

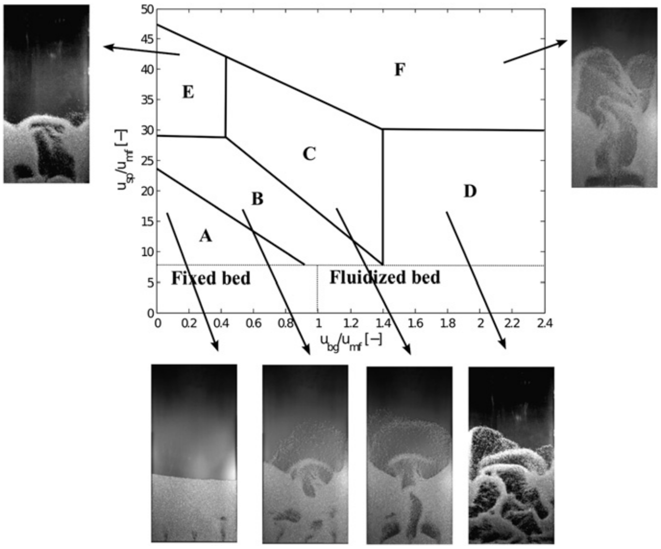

Fig. 7. Flow regime map with of multiple spout fluidized bed (of dimensions $W \times D \times H = 0.45 \times 0.02 \times 2.5\ \mathrm{m}^3$ with 3 mm glass beads and three identical spouts of size $0.01 \times 0.02\ \mathrm{m}^2$) with variation in background (u_{bg}) and spout velocity (u_{sp}), flow regimes as multiple-internal-spouts (A), multiple-spouts (B), multiple-interacting-spouts (C), multiple-jets-in-fluidized-bed (D), alternating-two-spout-contraction (E) and contracted-spouts-with-periodic-channel-blocking (F) regime (van Buijtenen et al., 2011b).

1. Before actual use of a spout fluidized bed for a given application, a flow regime map should be constructed to reduce future complications in operation and control. Furthermore, flow regime maps also help in understanding the hydrodynamics of the system which is of paramount importance for design and scale-up.
2. Up to now, flow regime maps are usually determined on basis of high-speed imaging and pressure drop measurements. However, in future efforts should be made to quantify variation in other bed properties, e.g. bed height, number of particle collisions, jet penetration length etc.
3. At present little information is available on flow regime transitions. Efforts should be made to reveal transition mechanisms. It

Table 2
Overview on representative studies which deals with investigation of flow regime map for spout fluidised beds.

Reference	Experimental set-up	Experimental technique	Regime terminology with selection criteria
Nagarkatti and Chatterjee (1974)	Experiments were carried out in a cylindrical spout fluidized bed reactor of 0.090 m diameter and various bed heights (108–185 mm) with 0.254–0.6 mm glass particles	Visual observation and pressure drop measurement	Packed, fluidized, spout, spout fluidized (spouting in the central part of reactor with fluidization in annulus), unstable spout, unstable spout fluidized (downward motion of particle with generation of spout)
Vukovic et al. (1984)	Experiments were carried out in a cylindrical spout fluidized bed of 0.07 m diameter and 1 m height with calcium carbonate particles of 1.8 mm diameter	They classified the regimes depending on the bed height, terminal settling velocity, spout and background velocity	Fixed bed, spout fluidized bed (the bed height is less than or equal to maximum spoutable bed height at minimum spout fluidized flow rate), spout fluidized bed (bed height is greater than maximum spoutable bed height at minimum spout fluidized flow rate), fluidized bed with local spout, spouted bed
Sutanto et al. (1985)	Half cylindrical bed of 0.15 m diameter with conical bottom of 60° inclination angle was used to investigate the flow regime map of three different particles as 2.9 mm polystyrene, 2.3 mm Millet and 3.9 mm high-density polyethylene	Visual observation were supported by pressure measurement	Fixed bed, jet in fluidized bed (This regime was observed when total flow rate is greater than flow rate at minimum fluidization. At higher background flow rate of particles behaves in slugging manner with 1–2 Hz frequency where as at lower back ground flow rate formation of bubble was observed), spouting with aeration(observed at lower background and higher spout velocity), spout fluidization(unstable spout with generation of bubbles near the top surface with 6–7 Hz frequency)
Link et al. (2005)	Experiments were performed in flat bottom 3D spout fluidized bed of $W \times D \times H$ of $0.154 \times 0.084 \times 1$ m^3 respectively with 2.5 mm glass beads	Visual observations were supported by high frequency analysis of obtained pressure drop signal with digital image recording	Fixed bed, internal spout, spouting with aeration(generation of spout with fluidization in annulus near to spout with 5–7 Hz frequency), slugging bed (particle move in slugging manner), spout fluidization (fluidization at top of the bed with slight movement of particles resulting in blocking of spout), jet-in-fluidized-bed (particles movement with continuous generation of bubbles in annulus)
Zhong et al. (2006d)	A Plexiglas rectangular spout fluidized bed of 0.3×0.3 m^2 cross-section and 2 m height with 90° cone angle was used with Geldart D particles of 3.2 mm Mung beans, 2.8 mm polystyrene beads (of diameter), 1.6 mm Millet and 1.3–2.3 mm glass beads	Visual observation were support by images captured by high resolution digital CCD camera	Internal jet, spouting, fluidizing, jet in fluidized bed with bubbling(spout formation with fluidization in upper section of bed), jet in fluidized bed with slugging (lager bubbles formation in the middle part of the reactor), spout fluidizing (unsteady spout with fluidised annular)
Zhang and Tang (2006)	Stainless steel cylindrical 0.125 m column with 1.2 m height and cone angle equal to 60° was used for quantification of flow regime map with 1.06–2.41 mm glass beads, 1.63 mm Millet and 3.24 mm EVA particles	Fourier transformation of pressure signal and quantitative comparing with combination of other parameter such as velocity of spout and minimum fluidization and Froude number	Fixed bed, spouting with aeration (observed at higher spout and lower background gas flow rate), spout fluidization (observed at high spout and background flow rates), jet in fluidized, slugging regime (at high background flow, coalescence of formed observed at the center of the bed resulting in formation of bigger bubble)
Zhong et al. (2009)	Experiments were performed in 0.1 m cylindrical bed with 2 m height under maximum operating pressure of 0.4 MPa, with 2.3 mm Millet particles	Digital image processing and Shannon entropy analysis were applied	Fixed bed, spouting with aeration, jet in fluidized with bubbling, jet in fluidized with slugging, spout fluidizing
van Buijtenen et al. (2011b)	Experiments were performed in pseudo 2D multi-spout fluidized bed reactor of $W \times D \times H$ of $0.45 \times 0.02 \times 2.5$ m^3 with 3 mm glass particles	Digital image analysis with Fourier transform of pressure drop fluctuations and positron emission particle tracking	Multiple internal spouts, multiple spouts, multiple interacting spouts, multiple jets-in fluidized bed, alternating two spout contraction, contracted spouts with periodic channel blocking

is anticipated that the interaction of the spout and bubbles plays crucial role in this respect.

3. Numerical studies

There are two main approaches to model spout fluidized beds: (i) the discrete particle model (DPM) and (ii) the two fluid model (TFM). The latter is usually based on the kinetic theory of granular flow (KTGF). A comprehensive discussion on various modeling strategies applied for the gas–solid flows can be found in van der Hoef et al. (2008), Deen et al. (2007), Shuyan et al. (2010), Zhong et al. (2006e). Here, we will only discuss the main features of the two modeling approaches and their specific strong and weak points related to modeling of spout fluidized beds.

In the discrete particle model (DPM) the dynamics of each individual particle is described by an equation of motion, whereas the gas phase hydrodynamics is described by the modified Navier Stokes equations. An accurate description of the particle motion requires incorporation of the gravity force, the drag force, the far field pressure force and the inter-particle contact forces. It is particularly important to have an accurate description of the drag force and the inter-particle force, since they dominate the particle dynamics. The drag force is traditionally described by a combination of the Ergun and Wen and Yu equations. However, in state-of-the-art DPM simulations these closure equations are often replaced by closures derived from independent detailed direct numerical (DNS) simulations (Koch and Hill, 2001; van der Hoef et al., 2005; Beetstra et al., 2007). The inter-particle force is usually characterized by a three-parameter model, which involves the normal and tangential coefficients of restitution and the coefficient of friction. Each of these coefficients can be determined experimentally for dry systems, as well as for wet systems (Antonyuk et al., 2009). Link et al. (2004) has shown for gas–solid flow in spout fluidized beds that the discrete particle model gives excellent predictions of the mean and fluctuating particle fluxes, provided that an appropriate drag closure is used. Recently, Ren et al. (2011) have reported DPM simulations of a 3D conical spout fluidized bed, which also include the lift force acting on the particles. Their work indicates that the lift force is of no importance in the annulus, where there is no opportunity for large velocity gradients to develop, whereas the lift force only has a minor effect in the spout. Link et al. (2004) carried out particle image velocimetry (PIV) measurements in a pseudo-2D bed to validate the model. It was found that the simulated particle time averaged and fluctuating particle flux patterns are in good agreement with the experimental data. To validate the model for a full 3D spout fluidized bed, Link et al. (2008) performed positron emission particle tracking (PEPT) measurements, whereas Link et al. (2009) made a comparison with optical fiber probe measurements. In all cases a very good correspondence with the experimental data was found, illustrating the power of the DPM model. Link et al. (2007) extended the DPM model to incorporate droplets for the modeling of spray granulation. They demonstrated that the model is well suited to study particle growth, because it inherently keeps track of distributions of particle properties, such as particle size, temperature and wetness. van Buijtenen et al. (2009a,2009b,2011a) studied the effect of particle wetness on the collisional particle behavior. The effective restitution coefficient depends strongly on the conditions under which a collision takes place. The main parameters are the liquid viscosity and film thickness, as well as the impact velocity. Under certain circumstances the restitution coefficient can reduce to zero, leading to sticking or agglomeration of particles. This has a profound impact on the overall bed behavior, leading to less mobile particles and locally very dense particle packing. This will eventually have as large impact on the product quality as well. Antonyuk et al. (2009) made an extensive study of the mechanisms at play during a wet collision, the results of which can directly be absorbed in DPM simulations. The DPM is very well suited to study the effect of geometrical changes to the spout fluidized bed, which was illustrated by van Buijtenen et al. (in press), who studied the effect of elevating the spout channel from the bottom of the bed. They performed DPM simulations for different geometrical configurations and compared the predictions with and experimental data obtained from PEPT, PIV and electrical capacitance tomography (ECT) measurements. They found that in the spout fluidization regime, an increase of the spout height leads to worse performance, since dead zones arise below the spout level. In the jet-in-fluidized-bed regime however, an increased spout height not only results in a decrease of the dead zones, but also increases the bed height and enhances the particle mixing.

In the two-fluid model (TFM) the dynamics of the particles are volume averaged, leading to continuum descriptions of both the gas and particle phases. This model was successfully applied by Zhong et al. (2006c,e,f,2007b,2010). The advantage of the TFM compared with the previous model is that one can model larger systems: the solids motion in each computational grid cells is characterized by a single solids phase velocity vector, whereas in the DPM one would need to keep track of the motion and collisions of $O(100)$ particles. The downside of the model is that the particle–particle collisions cannot be resolved by the model. Instead, these are accounted for through constitutive equations owing from the kinetic theory of granular flow (KTGF). The KTGF is well established for dense gas–solid systems, like spout fluidized beds. It should be noted here that the theory is only valid in the limit of nearly elastic collisions. Problems arise when the inter-particle collisions are strongly non-ideal. This is particularly the case for wet systems, like granulation and drying. That makes that one should be hesitant in applying the TFM to these kind of spout fluidized bed operations.

4. Discussion and recommendations

Based on the overview of experimental and numerical studies of spout fluidized beds, we have observed a number of challenges, namely:

1. Experimental investigations are often performed in transparent systems made of glass or polycarbonate to ensure visual observation, which may result in difficulties in investigations due to electrostatic forces between particles and walls. The particles in the bed either stick to the wall or to each other, resulting in difficulties in application of non intrusive measurement of particles velocity. This issue can be solved by humidifying the fluidizing gas, which considerably reduces the effect of static electric charging without measurable effect on the bed behavior (van Buijtenen, 2011c).
2. Particle velocities and fluxes are often quantified by using PIV/DIA techniques, which give acceptable velocity profiles in pseudo 2D geometries. But, particle behavior in 3D geometries should be performed by using other non-intrusive techniques such as PEPT. Moreover, particle image recording requires low light reflections from the bed wall. This can be achieved by using light sources directed at an angle lower than 45°. Here it should be noted that, the use of halogen lamps with high input power increases the bed temperature and leads to non-uniform distribution of light, which hampers DIA studies. In spout fluidized beds particles in the spout move much faster than in the annulus, making it difficult to select a proper time delay and exposure time for the recordings. However, the dynamic time range of PIV measurements is usually sufficiently large to ensure accurate velocity measurements in both regions. Typically time delays of 1 ms are used with exposure times of 0.5 ms. If the particle velocities in the spout are high this exposure time may lead to motion blurring in the images. In that case, one would need to reduce the exposure time even further.
3. In DPM simulations the contact forces during particle–wall and inter particle collisions are calculated with a soft sphere approach. In this approach particles are assumed to undergo deformation during contact where contact forces are quantified from a mechanical analogy involving a spring. The selection of the spring stiffness in normal and tangential directions plays an important role during simulations of spout fluidized bed with high spout velocity. Usually the spring stiffness is reduced such that the maximum particle overlap is less than 1% of the particle diameter.

The design in terms of ratio of bed diameter to spout diameter, bed aspect ratio, spout and background flow rate and geometrical configurations plays an imperative role in the particle dynamics and hence in the specific application. Based on the critical analysis of existing literature the following important design related information has been summarized:

1. In general, most experimental investigations have been performed on laboratory scale batch beds (either with flat or conical bottom) with maximum solid handling capacity in the rage of a few kilograms. Height and width of the bed have been maintained in the range of 0.1–1 m, but with depth and spout dimension (width and depth for flat bottom reactor) of the order of a few centimeters (large enough to avoid particle–wall interactions). This will ease non-intrusive experimental investigation such as quantification of velocity and solid volume

fraction. However, in order to have reliable design and scale up strategies, it is highly recommended to obtain related data for a 3D geometry with diameter exceeding 1 m, while considering various particle diameters and physical properties. Moreover, an effort should be directed to develop correlations for prediction of minimum spout and spout fluidization velocity, jet penetration length, and pressure drop at larger scales.

2. The distinguishing feature of the spout fluidized bed as compared to spouted and fluidized bed reactor is its flexibility in selection in spout and background flow rate. The spout and background velocities can be selected on the basis of a flow regime map, which gives an overall idea of the flow variation. In order to have a good gas–solid contact, the background velocity should be maintained higher than minimum fluidization velocity and then the appropriate spout velocity can be selected depending on pressure drop.
3. Hydrodynamic studies have generally been performed with mono-disperse particles under dry conditions. However in order to have a broader spectrum in design and scale up data, bed behavior should be analyzed with bi-, tri- and poly-disperse particles. Furthermore, the effect of particle–particle and particle–wall interactions on hydrodynamic behavior of the reactor should be determined under controlled liquid injection.
4. Spout fluidized beds are generally operated at high spout velocity, so it is necessary to investigate the effect of turbulence using suitable turbulence models.
5. Other geometrical configurations with vertical or horizontal baffles, multiple-spouts with and without draft tubes should be comprehensively studied to explore their applicability.

5. Conclusions

1. The minimum spout and spout-fluidization velocity increases with increasing bed height, particle and spout orifice diameter. The quantification of minimum spouting velocity plays an important role in the selection of inlet gas flow rate; hence it is necessary to have a unified correlation for the calculation of the minimum spouting velocity for various geometrical configurations. Here, it is difficult to recommend an appropriate correlation, due to the fact that it not only depends on the physical properties of the solids but also on the bed configuration. A small change in the configuration dramatically changes the minimum spout velocity. Also, it is not obvious to directly apply a correlation developed for one particular geometrical configuration to another configuration.
2. The pressure drop in a spout fluidized bed increases with increasing bed height, spout diameter and density of the particles, whereas it decreases with increasing particle diameter and spout gas velocity. Moreover, quantification of pressure drop can help in the selection of operating parameters, as well to provide sufficient information (after suitable analysis) about the generation and collapse of the bubbles. All this information can be used to gain insight in the flow behavior and its transitions.
3. Mixing in spout fluidized beds depends on the particle density, spout and background gas velocities. It is mainly attributed to diffusion, convective transport and circulation of particles due to formation and collapse of bubbles. As the spout gas velocity increase, particle circulation and gas mixing also increase, whereas increase in density results in lowering the mean cycle time. Furthermore, increase in background velocity results in lowering the mean cycle time leading to uniform residence time distribution and increase gas mixing at lower bed height. So, selection of background velocity is of utmost important to achieve uniform mixing conditions.
4. Identification of the flow regimes in spout fluidized beds can be achieved by visual observations or photographic analysis of captured images. However, it will be more effective to use pressure fluctuation signals in combination with a suitable analysis method e.g. fast Fourier transformation, Shannon entropy analysis, auto regressive model and wavelet transform to reinforce the identified flow regimes. Also, detailed analysis of the existing literature indicates the necessity of a comprehensive study of flow transitions.

Numerical models are important tools for investigating hydrodynamic behavior of spout fluidized beds. Future models should be extended to analyze the effect of restitution coefficient, wetness of particles and heat and mass transfer characteristics. In our view, the discrete particle model is the best learning model, as it best suited to describe the dynamics of wet particles.

Symbols

Roman letters

D	Depth of bed (m)
D_c	Effective column diameter (m)
D_{DT}	Draft tube diameter (m)
d_p	Particle diameter (m)
D_s	Nozzle/spout diameter (m)
Fr	Two-phase Froude number (dimensionless)
g	Acceleration due to gravity (m/s^2)
H	Total height of bed (m)
H_b	Bed height (m)
h_{sp}	Spout height (m)
L_j	Jet penetration length (m)
L_{DT}	Length of draft tube (m)
Q_{msf}	Minimum spout fluidizing flow rate (m^3/s)
$Q_{n,0,msf}$	Spout flow rate at bed inlet at Q_{msf} (m^3/s)
R	Entrainment height (m)
Re_p	Particle Reynolds number (dimensionless)
S	Ratio of Shannon entropy (dimensionless)
t	Time (s)
u_g	Superficial gas velocity (m/s)
u_{bg}	Background velocity (m/s)
u_{mf}	Minimum velocity for fluidization (m/s)
u_{msf}	Minimum spout fluidizing velocity (m/s)
u_{msDT}	Minimum spout velocity in draft tube (m/s)
u_{ms}	Minimum spout velocity (m/s)
u_{sp}	Spout velocity (m/s)
V_{cell}	Volume of grid cell (m^3)
V_p^i	Volume of particle (m^3)
W_c	Width of the bed (m)
W_s	Spout nozzle width (m)

Greek symbols

ρ_s	Absolute density of solid (kg/m^3)
ρ_g	Density of fluid (kg/m^3)
μ_g	Viscosity of gas (kg/m s)
ϕ	Function for bed height (dimensionless)
ϕ_s	Shericity of particle (dimensionless)
ε_m	Minimum solid volume fraction (dimensionless)
ε_g	Gas porosity (dimensionless)

Acknowledgments

This research is supported by the Dutch Technology Foundation STW, applied science division of NWO and the Technology

Program of the Ministry of Economic Affairs, as well by the DFG (German Research Foundation) in Germany. The authors would like to thank Tom van Hunsel for performing the pressure drop measurements.

References

Albina, D.O., 2006. Emissions from multiple-spouted and spout-fluid fluidized beds using rice husks as fuel. Renewable Energy 31, 2152–2163.

Anabtawi, M.Z., Uysal, B.Z., Jumah, R.Y., 1992. Flow characteristics in a rectangular spout-fluid bed. Powder Technol. 69, 205–211.

Anabtawi, M.Z., Hilal, N., Al Muftah, A.E., 2003. Volumetric mass transfer coefficient in non-Newtonian fluids in spouted-fluid beds: part I. Chem. Eng. Technol. 26, 759–764.

Anabtawi, M.Z., Hilal, N., Al Muftah, A.E., Leaper, M.C., 2004. Non-Newtonian fluids in spout-fluid beds: mass transfer coefficient at low Reynolds numbers. Particulate Sci. Technol. 22, 391–403.

Antonyuk, S., Heinrich, S., Deen, N.G., Kuipers, J.A.M., 2009. Influence of liquid layers on energy absorption during particle impact. Particuology 7, 245.

Beetstra, R., van der Hoef, M.A., Kuipers, J.A.M., 2007. Drag force of intermediate Reynolds number flow past mono- and bi-disperse arrays of spheres. AIChE J. 53, 48–501.

Bi, H.T., 2004. A discussion on minimum spout velocity and jet penetration length. Can. J. Chem. Eng. 82, 4–10.

Białobrzewski, I., Zielińska, M., Mujumdar, A.S., Markowski, M., 2008. Heat and mass transfer during drying of a bed of shrinking particles—simulation for carrot cubes dried in a spout-fluidized-bed drier. Int. J. Heat Mass Transfer 51, 4704–4716.

Börner, M., Peglow, M., Tsotsas, E., 2011. Particle, residence times in fluidized bed granulation equipments. Chem. Eng. Technol. 34, 1–8.

Chatterjee, A., 1970. Spout-fluid bed technique. Ind. Eng. Chem. Process Des. Dev. 9, 340–341.

Cheremisinoff, N.P., 1986. Review of experimental methods for studying the hydrodynamics of gas–solid fluidized beds. Ind. Eng. Chem. Process Des. Dev. 25, 329–351.

Ciro-Velásquez, H.J., Cunha, R.L., Menegalli, F.C., 2010. Drying of Xanthan gum using a two-dimensional spouted fluidized bed (2DSFB) with inert particles: performance and rheological considerations. Drying Technol. 28, 389–401.

Cui, H., Grace, J.R., 2008. Spouting of biomass particles: a review. Bioresour. Technol. 99, 4008–4020.

Deen, N.G., van Sint Annaland, M., van der Hoef, M.A., Kuipers, J.A.M., 2007. Review of discrete particle modeling of fluidized beds. Chem. Eng. Sci. 62, 28–44.

Dogan, O.M., Freitas, L.A.P., Lim, C.J., Grace, J.R., Luo, B., 2000. Hydrodynamics and stability of slot-rectangular spouted beds (part I: thin bed). Chem. Eng. Commun. 181, 225–242.

Ellis, N., Briens, L.A., Grace, J.R., Bi, H.T., Lim, C.J., 2003. Characteristics of dynamic behavior in gas–solid turbulent fluidized bed using chaos and wavelet analyses. Chem. Eng. J. 96, 105–116.

Epstein, N., Grace, J.R., 1996. Spouting of particulate solids. In: Fayed, M.E., Otten, L. (Eds.), Handbook of Powder Science and Technology, 2nd ed. Van Nostrand Reinhold Co., New York.

Fan, L.T., Kang, Y., Neogi, D., Yashima, M., 1993. Fractal analysis of fluidized particle behavior in liquid–solid fluidized bed. AIChE J. 39, 513–517.

Filla, M., Massimilla, L., Vaccaro, S., 1983. Gas jets in fluidized beds and spouts: a comparison of experimental behavior and models. Can. J. Che. Eng. 61, 370–376.

Gryczka, O., Heinrich, S., Miteva, V., Deen, N.G., Kuipers, J.A.M., Jacob, M., Morla, L., 2008. Characterization of the pneumatic behavior of a novel spouted bed apparatus with two adjustable gas inlets. Chem. Eng. Sci. 63, 791–814.

Gryczka, O., Heinrich, S., Deen, N.G., van Sint Annaland, M., Kuipers, J.A.M., Jacob, M., Morla, L., 2009. Characterization and CFD-modeling of the hydrodynamics of a prismatic spouted bed apparatus. Chem. Eng. Sci. 64, 3352–3375.

Jin, B.S., Zhou, S.M., Xiao, R., 2000. Experimental study on flow and diffusion characteristic in a pressurized spouted-fluidized bed. J. Combust. Sci. Technol. 6, 289–295.

Jin, B., Zhang, Y., Zhong, W., Xiao, R., 2009. Experimental study of the effect of particle density on mixing behavior in a spout-fluid bed. Ind. Eng. Chem. Res. 48, 10055–10064.

Kfuri, C.R., Freitas, L.A.P., 2005. A comparative study of spouted and spout-fluid beds for tablet coating. Drying Technol. 23, 2369–2387.

Knowlton, T.M., Hirsan, I., 1980. The effect of pressure on jet penetration in semi-cylindrical gas-fluidized bed. In: Grace, J.R., Matsen, J.M. (Eds.), Fluidization. Plenum, New York, pp. 315–324.

Koch, D.L., Hill, R.J., 2001. Inertial effects in suspension and porous-media flows. Annu. Rev. Fluid Mech. 33, 619–647.

Lefroy, G.A., Davidson, J.F., 1969. Trans. Inst. Chem. Eng. 47, T121.

Link, J., Zeilstra, C., Deen, N., Kuipers, H., 2004. Validation of a discrete particle model in a 2D spout-fluid bed using non-intrusive optical measuring techniques. Can. J. Chem. Eng. 82, 30–36.

Link, J.M., Cuypers, L.A., Deen, N.G., Kuipers, J.A.M., 2005. Flow regimes in a spout-fluid bed: a combined experimental and simulation study. Chem. Eng. Sci. 60, 3425–3442.

Link, J.M., Godlieb, W., Deen, N.G., Kuipers, J.A.M., 2007. Discrete element study of granulation in a spout-fluidized bed. Chem. Eng. Sci. 62, 195–207.

Link, J.M., Deen, N.G., Kuipers, J.A.M., Fan, X., Ingram, A., Parker, D., Wood, J., Seville, J., 2008. PEPT and discrete particle simulation study of spout-fluid bed regimes. Am. Inst. Chem. Eng. 54, 1189.

Link, J.M., Godlieb, W., Tripp, P., Deen, N.G., Heinrich, S., Kuipers, J.A.M., Schönherr, M., Peglow, M., 2009. Comparison of fiber optical measurements and discrete element simulations for the study of granulation in a spout fluidized bed. Powder Technol. 189, 202–217.

Littman, H., Paccione, J.D., Plawsky, J.L., 2009. New type of draft tube spout-fluid bed. Part 1: Hydraulic transport of 1.94 mm glass particles in water. Ind. Eng. Chem. Res. 48, 9286–9298.

Lopes da Cunha, R., Garća de la Cruz, A., Menegalli, F.C., 2006. Effects of operating conditions on the quality of mango pulp dried in a spout fluidized bed. Drying Technol. 24, 423–432.

Louge, M., 1997. Experimental techniques. In: Grace, J.R., Avidan, A.A., Knowlton, T.M. (Eds.), Circulating Fluidization Beds. Chapman & Hall, London, UK, pp. 312–368.

Lu, X., Li, H., 1999. Walete analysis of pressure fluctuation signals in a bubbling fluidized bed. Chem. Eng. J. 75, 113–119.

Marmo, L., 2007. Low temperature drying of pomace in spout and spout-fluid beds. J. Food Eng. 79, 1179–1190.

Marschall, K.-J., Mleczko, L., 2000. Experimental investigations of catalytic partial oxidation of methane to synthesis gas in various types of fluidized-bed reactors. Chem. Eng. Technol. 23, 31–37.

Mathur, K.B., Gishler, P.E., 1955. A technique for contacting gases with coarse solid particles. AIChE J. 1, 157–164.

Nagarkatti, A., Chatterjee, A., 1974. Pressure and flow characteristics of a gas phase spout-fluid bed and the minimum spout-fluid condition. Can. J. Chem. Eng. 52, 185–195.

Oliveira, W.P., Souza, C.R.F., Lim, C.J., Grace, J.R., 2008. Evaluation of flow regimes in a semi-cylindrical spouted bed through statistical, mutual information, spectral and Hurst's analysis. Can. J. Chem. Eng. 86, 582–596.

Osorio-Revilla, G., Lopez-Suarez, T., Gallardo- Velazquez, T., 2004. Simultaneous drying and cleaning of guava seeds in a spout-fluid bed with a draft tube. Can. J. Chem. Eng. 82, 148–153.

Park, K.-B., Plawsky, J.L., Littman, H., Paccione, J.D., 2006. Mortar properties obtained by dry premixing of cementitious materials and sand in a spout-fluid bed mixer. Cem. Concr. Res. 36, 728–734.

Pianarosa, D.L., Freitas, L.A.P., Lim, C.J., Grace, J.R., Dogan, O.M., 2000. Voidage and particle velocity profiles in a spout-fluid bed. Can. J. Chem. Eng. 78, 132–142.

Pimchuai, A., Dutta, A., Basu, P., 2010. Torrefaction of agriculture residue to enhance combustible properties. Energy Fuels 24, 4638–4645.

Plawsky, J.L., Jovanovic, S., Littman, H., Hover, K.C., Gerolimatos, S., Douglas, K., 2003. Exploring the effect of dry premixing of sand and cement on the mechanical properties of mortar. Cem. Concr. Res. 33, 255–264.

Plawsky, J.L., Littman, H., Paccione, J.D., 2010. Design, simulation, and performance of a draft tube spout fluid bed coating system for aerogel particles. Powder Technol. 199, 131–138.

Ren, B., Zhong, W., Jin, B., Yuan, Z., Lu, Y., 2011. Modeling of gas-particle turbulent flow in spout-fluid bed by computational fluid dynamics with discrete element method. Chem. Eng. Technol. 34, 2059–2068.

Saadevandi, B.A., Turton, R., 1998. The application of computer-based imaging to the measurements of particle velocity and voidage profiles in a fluidized bed. Powder Technol. 98, 183–189.

Shen, L., Wu, J., Gao, Z., Xiao, J., 2010. Characterization of chemical looping combustion of coal in a 1 kWth reactor with a nickel-based oxygen carrier. Combust. Flame 157, 934–942.

Shuyan, W., Zhenghua, H., Dan, S., Yikun, L., Lixin, W., Shuai, W., 2010. Hydrodynamic simulations of gas–solid spouted bed with a draft tube. Chem. Eng. Sci. 65, 1322–1333.

Sutanto, W., Epstein, N., Grace, J.R., 1985. Hydrodynamics of spout-fluid beds. Powder Technol. 44, 205–212.

Thamavithya, M., Dutta, A., 2008. An investigation of MSW gasification in a spout-fluid bed reactor. Fuel Process. Technol. 89, 949–957.

van Buijtenen, M.S., Deen, N.G., Heinrich, S., Antonyuk, S., Kuipers, J.A.M., 2009a. Discrete particle simulation study on the influence of the restitution coefficient on spout fluidized-bed dynamics. Chem. Eng. Technol. 32, 454–462.

van Buijtenen, M.S., Deen, N.G., Heinrich, S., Antonyuk, S., Kuipers, J.A.M., 2009b. A discrete element study of wet particle–particle interaction during granulation in a spout fluidized bed. Can. J. Chem. Eng. 87, 308–317.

van Buijtenen, M.S., Börner, M., Deen, N.G., Heinrich, S., Antonyuk, S., Kuipers, J.A.M., 2011a. An experimental study of the effect of collision properties on spout fluidized bed dynamics. Powder Technol. 206, 139–148.

van Buijtenen, M.S., Dijk, W.-J., Deen, N.G., Kuipers, J.A.M., Leadbeater, T., Parker, D.J., 2011b. Numerical and experimental study on multiple-spout fluidized beds. Chem. Eng. Sci. 66, 2368–2376.

van Buijtenen, M.S., 2011c. Multiphase Flow in Spout Fluidized Bed Granulators, Ph.D Thesis, Eindhoven University of Technology, The Netherlands.

van Buijtenen, M.S., Buist, K., Deen, N.G., Kuipers, J.A.M., Leadbeater, T., Parker, D.J., Numerical and experimental study on spout elevation in spout-fluidized beds, AIChE J., http://dx.doi.org/10.1002/aic.12765, in press.

van der Hoef, M.A., Beetstra, R., Kuipers, J.A.M., 2005. Lattice Boltzmann simulations of low Reynolds number flow past mono- and bi-disperse arrays of spheres: results for the permeability and drag force. J. Fluid Mech. 528, 233–254.

van der Hoef, M.A., van Sint Annaland, M., Deen, N.G., Kuipers, J.A.M., 2008. Numerical simulation of dense gas–solid fluidized beds: a multiscale modeling strategy. Annu. Rev. Fluid Mech. 40, 47–70.

van Ommen, J.R., Mudde, R.F., 2007. Measuring the gas–solids distribution in fluidized beds—a review. In: Proceedings of the 2007 ECI Conference on the 12th International Conference on Fluidization, New Horizons in Fluidization Engineering, pp. 31–45.

Vukovic, D.V., Hadzismajlovic, Dz.E., Grbavcic, Z.B., Garic, R.V., Littman, H., 1984. Flow regimes for spout-fluid beds. Can. J. Chem. Eng. 62, 825–829.

Wang, C.-H., Zhong, Z.-P., Li, R., Jia-Qiang, E., 2011. Intelligent fitting of minimum spout-fluidised velocity in spout-fluidised bed. Can. J. Chem. Eng. 89, 101–107.

Wang, G., Guo, W., Wang, H., Zhang, H., Zhang, Z., 1999. Hydrodynamics of draft tube spouted bed with aeration. J. Chem. Ind. Eng. 50, 637–643.

Werther, J., 1999. Measurement techniques in fluidized beds. Powder Technol. 102, 15–36.

Xiao, R., Zhang, M., Jin, B., Xiaong, Y., Zhou, H., Duan, Y., Zhong, Z., Chen, X., Shen, L., Huang, Y., 2007. Air blown partial gasification of coal in a pilot plant pressurized spout-fluid bed reactor. Fuel 86, 1631–1640.

Xie, Y., Xiao, J., Shen, L., Wang, J., Zhu, J., Hao, J., 2010. Effects of Ca-based catalysts on biomass gasification with steam in a circulating spout-fluid bed reactor. Energy Fuels 24, 3256–3261.

Xu, J., Bao, X., Wei, W., Shi, G., Shen, S., Bi, H.T., Grace, J.R., Lim, C.J., 2004. Statistical and frequency analysis of pressure fluctuations in spouted beds. Powder Technol. 140, 141–154.

Xu, J., Tang, J., Wei, W., Bao, X., 2009. Minimum spouting velocity in a spout-fluid bed with a draft tube. Can. J. Chem. Eng. 87, 274–278.

Yates, J.G., Simons, S.J.R., 1994. Experimental methods in fluidization research. Int. J. Multiphase Flow 20, 297–330.

Zhang, J., Tang, F., 2006. Prediction of flow regimes in spout-fluidized bed. China Particuol. 4, 189–193.

Zhang, M., 2005. Study on the Hydrodynamic Behavior of Spout-Fluid Bed with a Draft Tube, Master Thesis, Tianjin University, China.

Zhang, Y., Jin, B., Zhong, W., 2008. Experimental Investigations on the effect of the tracer location on mixing in a spout-fluid bed. Int. J. Chem. React. Eng. 6, A46.

Zhang, Y., Jin, B.S., Zhong, W.Q., 2009a. Experiment on particle mixing in flat-bottom spout fluid bed. Chem. Eng. Process 48, 126–134.

Zhang, Y., Jin, B., Zhong, W., Ren, B., Xiao, R., 2010. DEM simulation of particle mixing in flat-bottom spout-fluid bed. Chem. Eng. Res. Des. 88, 757–771.

Zhang, Y., Zhong, W., Jin, B., 2011. New method for the investigation of particle mixing dynamic in a spout-fluid bed. Powder Technol. 208, 702–712.

Zhong, W., Zhang, M., 2005a. Jet penetration depth in a two-dimensional spout-fluid bed. Chem. Eng. Sci. 60, 315–327.

Zhong, W., Zhang, M., 2005b. Characterization of dynamic behavior of a spout-fluid bed with Shannon entropy analysis. Powder Technol. 159, 121–126.

Zhong, W., Zhang, M., 2005c. Pressure fluctuation frequency characteristics in a spout-fluid bed by modern ARM power spectrum analysis. Powder Technol. 152, 52–61.

Zhong, W., Zhang, M., Jin, B., 2006a. Maximum spoutable bed height of spout-fluid bed. Chem. Eng. J. 124, 55–62.

Zhong, W., Chen, X., Zhang, M., 2006b. Hydrodynamic characteristics of spout-fluid bed: pressure drop and minimum spouting/spout-fluidizing velocity. Chem. Eng. J. 118, 37–46.

Zhong, W., Xiao, R., Zhang, M., 2006c. Experimental study of gas mixing in a spout-fluid bed. AIChE J. 52, 924–930.

Zhong, W., Zhang., M., Jin, B., Chen, X., 2006d. Flow pattern and transition of rectangular spout-fluid bed. Chem. Eng. Process. 45, 734–746.

Zhong, W., Xiong, Y., Yuan, Z., Zhang, M., 2006e. DEM simulation of gas–solid flow behaviours in spout-fluid bed. Chem. Eng. Sci. 61, 1571–1584.

Zhong, W., Zhang, M., Jin, B., Yuan, Z., 2006f. Three-dimensional simulation of gas/solid flow in spout-fluid beds with kinetic theory of granular flow. Chin. J. Chem. Eng. 14, 611–617.

Zhong, W., Zhang, M., Jin, B., Zhang, Y., Xiao, R., Huang, Y., 2007a. Experimental investigation of particle mixing behavior in a large spout-fluid bed. Chem. Eng. Process. 46, 990–995.

Zhong, W., Zhang, M., Jin, B., Yuan, Z., 2007b. Flow behavior of a large spout-fluid bed at high pressure and temperature by 3D simulation with kinetic theory of granular flow. Powder Technol. 175, 90–103.

Zhong, W., Li, Q., Zhang, M., Jin, B., Xiao, R., Huang, Y., Shi, A., 2008. Spout characteristics of a cylindrical spout-fluid bed with elevated pressure. Chem. Eng. J. 139, 42–47.

Zhong, W., Wang, X., Li, Q., Jin, B., Zhang, M., Xiao, R., Huang, Y., 2009. Analysis on chaotic nature of a pressurized spout-fluid bed by information theory based Shannon entropy. Can. J. Chem. Eng. 87, 220–227.

Zhong, W., Zhang, Y., Jin, B., 2010. Novel method to study the particle circulation in a flat-bottom spout-fluid bed. Energy Fuels 24, 5131–5138.

Zhong, W., Jin, B., Zhang, M., Xiao, R., 2011. Hydrodynamics of Spout-Fluid Beds, Chapter 6, Page 105–127 in Spouted and Spout-Fluid Beds. In: Epstein, N., Grace, J.R. (Eds.), Cambridge University Press.

Zielinska, M., Markowski, M., 2007. Drying behavior of carrots dried in a spout-fluidized bed dryer. Drying Technol. 25, 261–270.